

Identification of Molecular Crystals Capable of Undergoing an Acyl-Transfer Reaction Based on Intermolecular Interactions in the Crystal Lattice

Majid I. Tamboli,^[a] Shobhana Krishnaswamy,^[b] Rajesh G. Gonnade,^[b] and Mysore S. Shashidhar*^[a]

Abstract: Investigation of the intermolecular acyl-transfer reactivity in molecular crystals of *myo*-inositol ortho-ester derivatives and its correlation with crystal structures enabled us to identify the essential parameters to support efficient acyl-transfer reactions in crystals: 1) the favorable geometry of the nucleophile (–OH) and the electrophile (C=O) and 2) the molecular assembly, reinforced by C–H⋯π interactions, which supports a domino-type

reaction in crystals. These parameters were used to identify another reactive crystal through a data-mining study of the Cambridge Structural Database. A 2:1 co-crystal of 2,3-naphthalene diol and its di-*p*-methylbenzoate was select-

ed as a potentially reactive crystal and its reactivity was tested by heating the co-crystals in the presence of solid sodium carbonate. A facile intermolecular *p*-toluoyl group transfer was observed as predicted. The successful identification of reactive crystals opens up a new method for the detection of molecular crystals capable of exhibiting acyl-transfer reactivity.

Keywords: acylation • domino reactions • intermolecular interactions • solid-state reactions • X-ray diffraction

Introduction

Carbon–carbon and carbon–heteroatom (O, N, S) bond-forming reactions in molecular crystals have been investigated in the last few decades because of their facility and often, unique product selectivity.^[1–6] The crystal lattice provides a structured environment for specific reactions, which results in high product selectivity compared with the corresponding solution-state reactions. Reactions in solids, apart from being potential environmentally green or benign reaction systems, also contribute to the understanding of differences in the stability of small molecules in different phases, including drug formulations.^[7–10] The pioneering work of Schmidt^[11–13] and later others^[14–19] helped formulate requirements in terms of inter-atomic distances, design and create templates and new substrates for the addition reactions of olefins in crystals, resulting in C–C bond formation. In contrast, most of the reports on reactions in molecular crystals involving migration of relatively larger group of atoms between the reacting centers have been sporadic stand-alone

examples.^[20–24] This is perhaps because most of these reactive crystals were comprised of one chemical entity and hence the reactions investigated were either intramolecular reactions or homomolecular reactions (implying reactions between one kind of molecules).

Transesterification reactions, involving nucleophilic addition to carbonyl groups (followed by elimination), are frequently encountered organic reactions in the solution state and in living systems. Acyl group-transfer reactions, albeit few, have also been reported to occur in the organic solid-state.^[7–9,25,26] The earliest report was the thermally induced intramolecular O→N acyl migration in *O*-acylsalicylamide.^[25] Vyas and co-workers correlated the facile intramolecular acyl group migration with the geometry of the reactive centers in the crystalline state.^[26] Transacylation was also observed in tablet mixtures of aspirin and drugs with easily acylated functionalities such as phenylephrine hydrochloride, codeine, and acetaminophen.^[7–9] We had reported (the first instance^[27] of) a facile intermolecular benzoyl group transfer in crystals of racemic 2,4-di-*O*-benzoyl-*myo*-inositol 1,3,5-orthoformate (**1**), its orthoacetate analogue **2**,^[28] as well as in co-crystals **1**·**2**^[29] (Scheme 1), which yielded the corresponding tribenzoates **3** and **4** and the diols **5** and **6**.

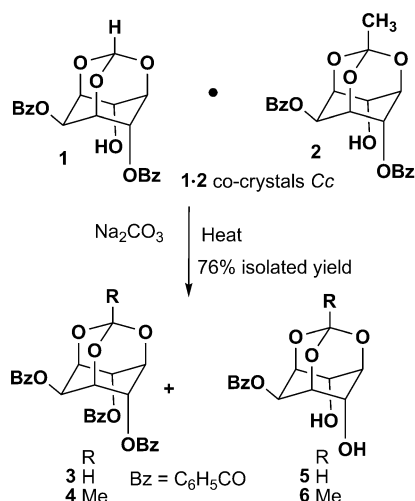
A comparison of the crystal structures of all the compounds in which the intermolecular acyl-transfer reaction occurred and their polymorphs in which the corresponding reaction was not facile, helped us determine the minimum conditions necessary for the occurrence of intermolecular acyl-transfer reaction in molecular crystals.^[30,31] The present article reports identification of a molecular co-crystal (in the light of prior knowledge generated in our laboratory), by

[a] M. I. Tamboli,* Dr. M. S. Shashidhar
Division of Organic Chemistry, CSIR–National Chemical Laboratory
Dr. Homi Bhabha Road, Pashan, Pune-411008 (India)
Fax: (+91)20-25902629
E-mail: ms.shashidhar@ncl.res.in

[b] Dr. S. Krishnaswamy,* Dr. R. G. Gonnade
Center for Materials Characterization
CSIR–National Chemical Laboratory, Dr. Homi Bhabha Road
Pashan, Pune-411008 (India)

[*] These authors contributed equally to this work.

Supporting information for this article is available on the WWW under <http://dx.doi.org/10.1002/chem.201301058>.



Scheme 1. Solid-state transesterification reactions in co-crystal **1·2** of *myo*-inositol orthoester derivatives.

search of the Cambridge Structural Database (CSD, Version 5.34, November 2012), which had the potential to support intermolecular acyl-transfer between its constituent molecules and the experimental verification of the facility of acyl-transfer reaction as anticipated.

A large body of data on reactions in solutions, accumulated over more than a century, helped chemists to categorize organic reactions in terms of “functional groups” and hence increased the probability of fairly accurate prediction of the facility of reactions of organic molecules and the structure of the possible products, based on the structure of the reactant molecules. In contrast, the complex nature of non-covalent intermolecular interactions precludes the design and synthesis of crystals that contain the reactive centers (of constituent molecules) in the right relative orientation for successful covalent bond formation. The prevalence of polymorphic modifications and their thermal phase transitions in the solid state also contribute to the uncertainty in prediction of the reactivity of molecules in their crystals. The results presented here show that the knowledge generated by systematic analysis of crystal structures that facilitate a chemical reaction, can be utilized in identifying other reactive crystalline solids.

Results and Discussion

Efficient intermolecular oxygen-to-oxygen benzoyl group-transfer reactions were observed in *myo*-inositol orthoester derivatives **1**, **2**, and co-crystals **1·2**. Single-crystal X-ray diffraction analysis of these reactive crystals^[28,29] revealed that the distance between the reaction centers (HO...C=O), and the angle of approach of the -OH (nucleophile = Nu) towards the ester carbonyl group, C=O (electrophile = El) lay in the range of 3.1–3.3 Å and 84–90°, respectively.^[28] These interatomic distances and angles are close to those arrived for El...Nu interactions through the study of crystal struc-

tures and theoretical calculations on a model system, by Bürgi and Dunitz.^[32] Their results (from crystal structure data) indicated that the N...C=O and O...C=O angles were in the range (105 ± 5)° for all the distances smaller than 2.5 Å between the electrophile and the nucleophile. Hydroxy acids with intramolecular O...C=O angles of ≈ 98° show the highest rate of intramolecular lactonization^[33] and Bender^[34] also postulated that a perpendicular approach of the nucleophile to the π-electron system should be preferred over a coplanar approach in order to maximize the overlap between the nucleophile and π-electrons of the carboxyl group during intramolecular lactonization. Hence, it is reasonable to expect larger deviation of O...C=O angle (from the tetrahedral angle) as the El...Nu distance increases (beyond 2.5 Å), as observed in reactive crystals of *myo*-inositol orthoester derivatives. Subsequent investigations of structure and benzoyl group-transfer reactions in crystals of other *myo*-inositol 1,3,5-orthoester derivatives^[29–31] helped us realize the importance of helical molecular pre-organization in reactive crystals,^[35] which functions as a reaction channel and contributes to the facility and almost quantitative conversion of the reactants to products. Hence, we wondered whether 1) El...Nu geometry between potentially reactive centers in molecules; 2) the assembly of these reacting pairs in the crystal, in the form of a channel for the reaction to propagate; and 3) weak intermolecular interactions,^[36,37] such as C–H...π,^[38,39] which help maintain the topochemical control, could be used as parameters to predict the facility of acyl group-transfer reactivity in molecular crystals.

A survey of the CSD for compounds containing a carbonyl group and an oxygen nucleophile revealed that when the distance between the electrophile and the nucleophile was lesser than the sum of their van der Waals radii (3.22 Å), the angle of approach of the nucleophile towards the electrophile lay mostly in the range of 80–100°.^[31] The CSD searches, depending on the distance between the ester carbonyl carbon (El) and the hydroxyl oxygen (Nu) (HO...C=O, 3.1–3.5 Å, defined as a non-bonded contact) and the corresponding angle (85–95°, see Figure 1), yielded ≈ 200 hits. About 100 of these structures were scrutinized and ten of these were selected as “potentially reactive” crystals.^[40–49] The co-crystal **7·8** (CSD reference code: IJAGIJ) was

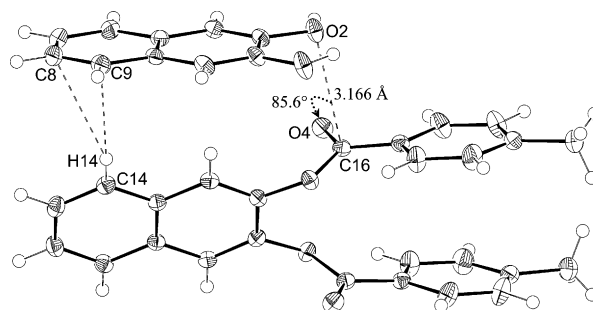


Figure 1. Relative orientation of the neighboring molecules of **7** and **8** in co-crystals **7·8** at -173°C. Thermal ellipsoids are drawn at 50% probability level and H-atoms are depicted as spheres of arbitrary radii.

chosen for the actual experiment due to its ease of preparation in larger amounts and also due to contemporary interest in the preparation and the study of properties of co-crystals. The grounds for rejection of other “hits” in the CSD were 1) crystal comprising of one kind of molecule (i.e., El and Nu present in the same molecule) since we had earlier reported^[27,28] reactions in such crystals; 2) solvated crystal: Potential loss of solvent and hence possibility of phase change on heating, which could make the structure–reactivity correlation difficult; 3) multistep synthesis for obtaining the desired molecule and hence its crystal; 4) compound obtained by isolation in small quantities from natural sources; 5) hydrated crystal: Potential loss of water and/or possibility of hydrolysis during the acyl-transfer reaction in crystals. In the 2:1 co-crystal **7·8** of 2,3-naphthalene-diol (**7**) and its di-*p*-methylbenzoate (**8**) the distance between the nearest Nu (–OH of **7**) and the El (C=O of **8**) was 3.166 Å and the angle of approach of Nu towards El was 85.6° (Figure 1; for similar association at higher temperatures, see Figure S1–S4, the Supporting Information).

A view of the crystal packing along the *ab*-diagonal (Figure 2a) revealed a layered structure in which the naphthalene rings of **7** and **8** are perpendicular to each other. Such a molecular assembly brings the hydroxyl oxygen (Nu) of the diol **7** in close proximity to the carbonyl carbon (El) of the adjacent diester **8**, and generates a short El··Nu contact (O2··C16=O4), satisfying one of the pre-requisites for the acyl group migration from **8** to **7** (Figure 1 and Table 1).

Table 1. El··Nu parameters for the reacting molecules in the co-crystal **7·8** at various temperatures.

El··Nu	–173	25	100	125	25 ^[a]
C16··O2	3.162	3.272	3.341	3.269	3.277
∠O4=C16··O2	85.8	84.6	84.4	84.7	84.5
∠H2A–O2··C16	82	84	85	82	84
∠C3–O2··C16	102.4	101.3	100.7	101.3	101.1

[a] Crystal was heated to 136°C on hot-stage microscope and then cooled to 25°C.

This molecular architecture is further supported by the formation of off-centered C–H·· π interactions involving naphthalene ring protons of the diester **8** and π -cloud of the adjacent diol **7** molecules (Figure 2a, for color graphic see Figure S5, the Supporting Information). The neighboring layers are connected to each other through strong intermolecular O–H··O hydrogen bonds (O2–H2A··O4), and linear C–H··O (C18–H18··O1) interactions (Table S2, the Supporting Information), thus providing well-directed discrete reaction channels throughout the crystal lattice (Figure 2b and 2c; for a color graphic see Figure S5, the Supporting Information). Hence, the co-crystal **7·8** had all the structural features (see points (1)–(3) mentioned earlier), for an intermolecular *p*-toluoyl group-transfer reaction between **7** and **8** (Scheme 2).

The experiment for verifying the expected reactivity in co-crystals **7·8** was interesting because the structure of the

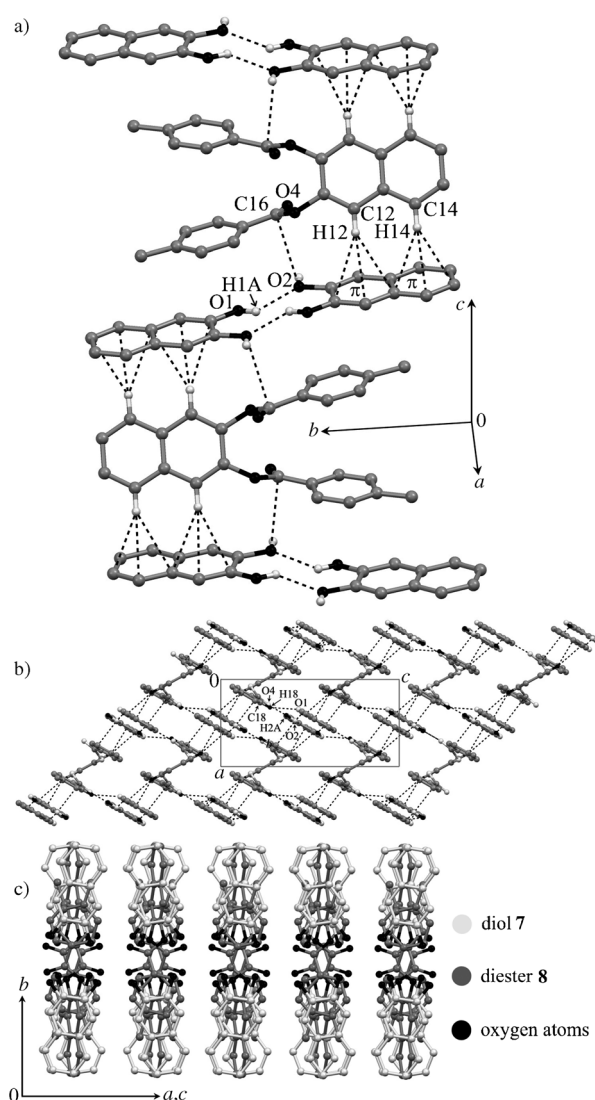
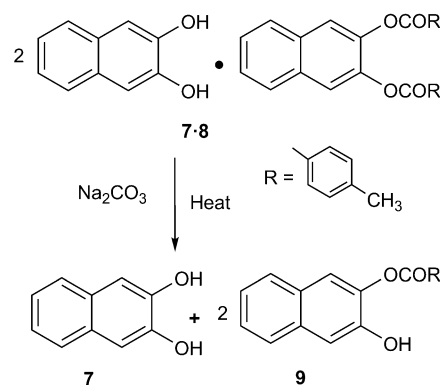


Figure 2. Packing of molecules in co-crystal **7·8**. a) Layered structure of molecules in crystals **7·8** displaying a sandwiched arrangement of diol molecules between the diesters; b) molecular packing viewed down the *b* axis revealing bridging of neighboring reactive layers through strong O–H··O and C–H··O interactions; c) view of the packing of molecules down the reaction channel showing discrete alignment of the layers.



Scheme 2. Intermolecular toluoyl group transfer in co-crystals **7·8**.

constituent molecules (inositol orthoester derivatives) of crystals that were used to arrive at the necessary conditions for acyl transfer are hugely different from the constituent molecules (naphthalene derivatives) of co-crystals **7·8** in which the reaction was expected to occur.

The acyl-transfer reactivity in **7·8** was tested as described in the experimental section to isolate the *p*-toluate **9** in a very good yield (91%). Since the diol **7** and the diester **8** are present in the molar ratio of 2:1 in the co-crystal, ≈ 1 equivalent of the diol **7** was also obtained at the end of the reaction. No acyl-transfer reactivity was observed at temperatures below 110°C or in the absence of sodium carbonate. The acyl-transfer reaction was less efficient above the melting point of co-crystals **7·8** (140–145°C, 5 h, 46% yield of **9**) as compared to the reaction below the melting point (122–125°C, 6 h, 80% yield of **9**). Isolation of *p*-toluic acid as one of the products in the reaction above the melting point of the co-crystals **7·8** indicated that the acyl-transfer reaction was less specific in the molten state (due to loss of topochemical control) and was accompanied by hydrolysis of the ester group. The diester **8** predominantly underwent hydrolysis in DMF solution, when allowed to react with **7** in the presence of sodium carbonate. Use of *p*-xylene as the solvent resulted in the formation of the monotoluic acid **9** (9%) and about 40% of the unreacted **8** was recovered. A comparison of all these results clearly indicates the role played by the crystal lattice during the reaction between **7** and **8** in their co-crystals.

The co-crystal **7·8** was reported^[42] as an intermediate in the solvent-free acylation of the diol **7** with *p*-toluoyl chloride at or below 125°C. The existence of this intermediate in the reaction mixture was revealed by IR spectroscopy, and the same intermediate was later crystallized using **7** and **8**. Although the co-crystal **7·8** was described as an intermediate during the O-acylation of **7**, it was not clear whether co-crystals **7·8** functioned as reactive intermediates during the solvent free acylation of **7** with *p*-toluoyl chloride. This is especially because the solvent free benzoylation of **7** with *p*-toluoyl chloride at 120°C was complete in 15 min to yield the diester **8**. The acyl-transfer reaction in co-crystals **7·8** on the other hand, needed several hours above 120°C for completion. Hence it is unlikely that the acylation of **7** under solvent free conditions proceeded exclusively through a topochemically controlled benzoyl group-transfer reaction in the intermediate co-crystals **7·8**.

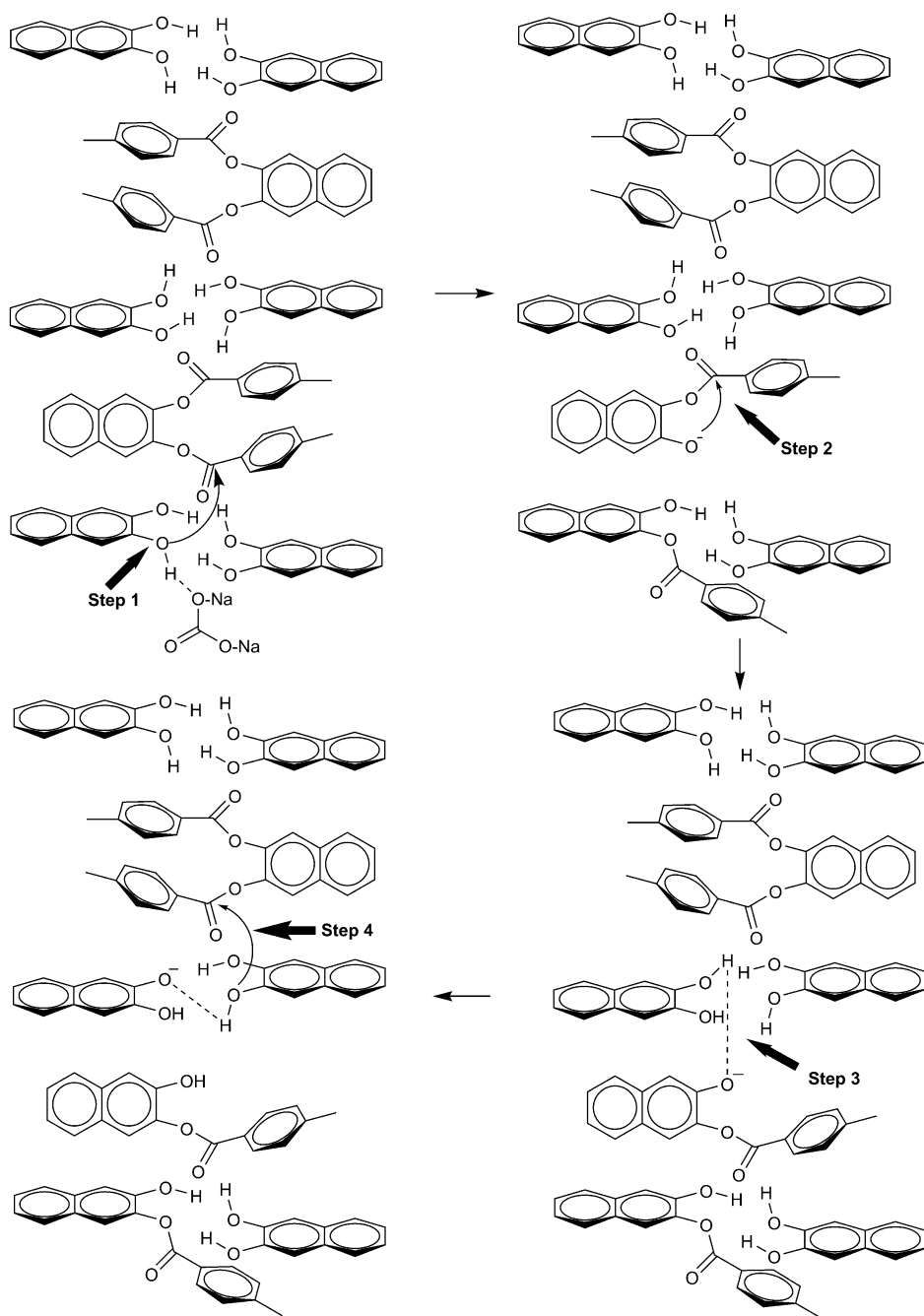
The facile formation of co-crystals **7·8** just by co-grinding the diol **7** and its diester **8** revealed a strong affinity between these two molecules (Figure S13, the Supporting Information). The significant interactions observed between **7** and **8** in their co-crystals were, (i) O–H...O hydrogen-bonding interactions between OH of the diol **7** and the C=O group of **8**; (ii) short El (C=O) and Nu (OH) contact; (iii) C–H...O contacts and (iv) C–H... π interactions between the naphthalene ring proton of **8** and aromatic ring of the diol **7** (Table S2, the Supporting Information). An estimation of the lattice energy^[50] of the co-crystal **7·8** gave a value of -233 kJ mol^{-1} . The computation of interaction energies for

significant interactions between **7** and **8** revealed comparable values for H–O...C=O, that is, El...Nu contact ($-67.8 \text{ kJ mol}^{-1}$) and O–H...O hydrogen-bonding interaction ($-70.7 \text{ kJ mol}^{-1}$), whereas, interaction energies for C–H...O ($-19.6 \text{ kJ mol}^{-1}$) and C–H... π contacts (-5.3 kJ mol^{-1}) were noticeably lower. These values reveal the relative importance of the El...Nu contacts (O2...C16=O4) in the layered arrangement of one diester **8** and two diol **7** molecules (Figure 2) in co-crystals **7·8**.

The El...Nu parameters as well as the molecular assemblies shown in Figures 1 and 2 are derived from the X-ray diffraction data of co-crystals **7·8** collected at low temperature. However, the acyl-transfer reaction in **7·8** occurred at much higher temperature. Hence, we wanted to observe the effect of temperature on the crucial intermolecular interactions shown in Figures 1 and 2. The X-ray diffraction intensity data measurement at 100°C was carried out successfully, however data collection at temperatures higher than 100°C was not initially successful due to changes at the crystal surface (Figure S7, the Supporting Information) leading to fragmentation of the exterior into small crystallites (the interior of the crystal was intact). The diffraction spots confirmed the single crystalline nature but high mosaicity and bad least-squares of the orientation matrix suggested a phase change (this could be responsible for a small endothermic hump in the differential scanning calorimetry (DSC) of **7·8** prior to melting, Figure S12, the Supporting Information). Removal of the small crystallites from the surface and rapid collection of the data sets (at 125°C) gave the structure of the co-crystal **7·8** with a good R-value. We also determined the structure of the co-crystal **7·8** (at 25 (2)°C), which was heated up to 136°C (close to melting temperature 139°C) on hot stage polarizing microscope and then cooled to room temperature. The structure overlay of the reacting molecules at different temperatures matched very well (Figure S6, the Supporting Information).

These experiments revealed that there were no major changes in the intermolecular El...Nu contacts, with variation in temperature (Figure 1 and Table 1). The variable temperature powder X-ray diffraction patterns recorded at temperatures of 25, 80, and 125°C matched reasonably well (Figures S14–S17, the Supporting Information), thus suggesting a modest effect of heating on the packing arrangements of molecules in the crystal lattice of co-crystals **7·8**. Interestingly, the thermal anisotropies of molecules of **7** and **8** in co-crystals **7·8** at 100°C showed a significant change; the lone pair on the oxygen of the hydroxyl group was found to be better oriented towards the carbonyl carbon, as compared with that observed at other temperatures (Figure 1 and Figures S1–S4, the Supporting Information). The thermal motion analysis of the reactants revealed a larger internal motion of O2 towards C16 at 100°C. This motion diminished at 125°C suggesting stabilization of the movement of these groups towards each other at higher temperatures. This perhaps implies the onset of the acyl-transfer reaction between **7** and **8** in co-crystals **7·8**.

The mechanism of the acyl-transfer reaction depicted in Scheme 3 rationalizes the experimentally observed high extent of conversion of reactants to product. Sodium carbonate possibly initiates the reaction at the base of a molecular layer (Step 1, Scheme 3) after which the reaction progresses by successive proton and *p*-toluoyl group transfers, resulting in a clean reaction and high yield of the mono ester **9**. A high percentage of conversion of reactants to products observed is consistent with this mechanism since the acyl-transfer reaction initiated at the surface of the crystals by the base (sodium carbonate, Step 1, Scheme 3) can



Scheme 3. A mechanism for the acyl group transfer from **8** to **7** in **7·8**.

progress well into the crystal, by generation of phenoxide ions due to a series of intramolecular toluoyl group transfer (Step 2, Scheme 3) and proton transfer (Steps 3 and 4, Scheme 3).

The intramolecular toluoyl group transfer proposed in Step 2 of Scheme 3 is supported by the perpendicular approach of the phenolic oxygen (Nu) of **8** towards the ester carbonyl group (C=O, E1) of the same molecule (Figure 3, for a color graphic see Figure S10, the Supporting Information). The E1...Nu distance observed in the crystal of **7·8** for intramolecular toluoyl group transfer is 2.935(2) Å and the angle of approach is 80.9°. The intramolecular transfer of the toluoyl group is necessary to sustain a domino-type reaction in co-crystals **7·8**.

We also solved the crystal structure of the product **9** (Figure S8, Table S1, the Supporting Information) for comparison with the structure of the co-crystal **7·8** and to inspect the E1...Nu geometry for inter- as well as intramolecular acyl-transfer. The intramolecular geometry (E1...Nu distance O2...C11=2.937 Å and angle O2...C11-O3=80.9°) for acyl transfer in crystals of the mono-ester **9** matches (Figure 4; for a color graphic see Figure S11, the Supporting Information) with the parameters observed for the diester **8** in its co-crystal **7·8**, supporting the possibility of intramolecular acyl-transfer during the process shown in Scheme 3.

However, a catemeric association of the *c*-glide-related molecules through strong O-H...O (O2-H2A...O3) hydrogen-bonding interactions between the carbonyl oxygen atom and the hydroxyl group (potential reaction centers) of adjacent molecules precludes the possibility of intermolecular acyl-transfer reaction in crystals of **9** (Figure S9, Table S3, the Supporting Information).

Conclusion

Co-crystals and molecular complexes have gained prominence

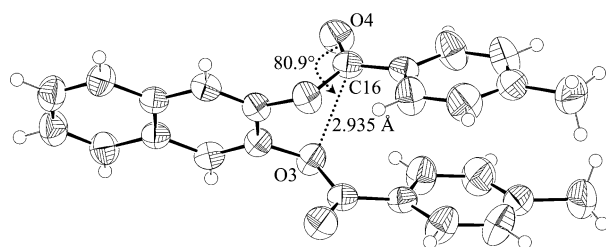


Figure 3. ORTEP of the diester **8** in a crystal of **7·8** showing relative orientation between the phenolic oxygen and ester carbonyl group at 125°C. Thermal ellipsoids are drawn at 50% probability level and H-atoms are depicted as spheres of arbitrary radii.

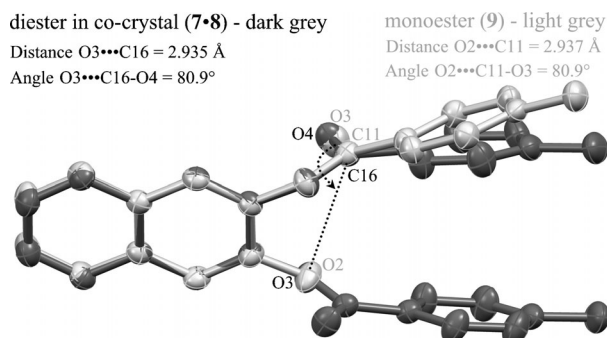


Figure 4. Molecular overlap of the diester **8** in a crystal of **7·8** and **9** in its crystal.

in the last two decades with numerous studies devoted to developing methods of synthesis and potential applications.^[51–60] Solid-state reactions in such multi-component crystals are rare and constitute a largely unexplored field due to inherent difficulties in obtaining molecular crystals wherein the reacting centers are aligned in the proper orientation for the desired reaction. Our investigations illustrate the importance of systematic studies of group transfer reactions in crystals paving the way for identification of reactive crystals and co-crystals from the crystal structure database. This provides a new route to obtain crystals that are capable of undergoing chemical reactions. Structure–reactivity correlation studies in crystals could also provide methods for evaluating the chemical stability of functional multicomponent solids.

Experimental Section

Crystallization: Naphthalene-2,3-diol (**7**, 0.32 g, 2 mmol) and its di-*p*-methyl benzoate^[42] **8** (0.396 g, 1 mmol) were dissolved in ethyl acetate (10 mL) by warming; light petroleum (90 mL) was added and the resulting solution was stored in an open container, at ambient temperature. Crystallization was complete in a few hours to yield the 2:1 co-crystals **7·8** (0.716 g), M.p. 139–140°C. The structure of the co-crystals **7·8** revealed by single-crystal X-ray diffraction analysis was identical to that retrieved from the CSD.^[42] Crystallization of a mixture of **7** and **8** in the molar ratio 1:1 or 1:2 or 1:3 also yielded 2:1 co-crystals **7·8** consistently. The co-crystals **7·8** could also be obtained by grinding a mixture of the

diol **7** (0.160 g, 1.0 mmol), the diester **8** (0.198 g, 0.50 mmol), and two–three drops of ethyl acetate, using a pestle and mortar.

Solid-state reactivity of co-crystals 7·8: A mixture of freshly grown crystals of **7·8** (0.093 g, 0.13 mmol) and activated sodium carbonate (0.110 g, 1.03 mmol) was ground into a fine powder using a mortar and pestle. The mixture was transferred to a test tube filled with argon, and heated in an oil bath (122–125°C) for 60 h. The reaction mixture was cooled to ambient temperature, suspended in water (20–30 mL) and then extracted with ethyl acetate (20–30 mL). The organic extract was washed with water, followed by brine. The organic layer was dried over anhydrous sodium sulphate and evaporated under reduced pressure. The residue obtained was purified by column chromatography (silica gel 100–200 mesh; eluent, ethyl acetate/light petroleum 10:90, v/v) to obtain **9** (0.066 g, 91%) as a solid. M.p. 197–198°C (crystals from chloroform); TLC (35:65 ethyl acetate/light petroleum, v/v); R_f : 0.6; $^1\text{H NMR}$ (200 MHz, CDCl_3): δ = 8.12–8.20 (m, 2H), 7.69–7.80 (m, 3H), 7.30–7.50 (m, 5H), 5.70 (s, 1H), 2.48 ppm (s, 3H); $^{13}\text{C NMR}$ (50 MHz, $[\text{D}_6]\text{Acetone}$): δ = 165.7, 149.7, 145.6, 141.8, 134.2, 131.3, 130.5, 129.6, 128.4, 128.2, 127.2, 127.1, 124.9, 121.9, 112.3, 22.0 ppm; IR (Nujol): $\tilde{\nu}$ = 3391, 1723 cm^{-1} ; elemental analysis calcd (%) for $\text{C}_{17}\text{H}_{24}\text{O}_3$: C 77.68, H 5.07; found: C 77.30, H 4.81. The diol **7** (0.022 g, 53%) was recovered on elution with ethyl acetate/light petroleum (25:75 v/v) (Figures S18–S22, the Supporting Information).

Reaction of 7·8 in melt: The co-crystals **7·8** (0.179 g, 0.25 mmol) and sodium carbonate (0.212 g, 2 mmol) were ground together. The mixture obtained was placed in a test tube and immersed in an oil bath preheated to 145°C (reaction time 5 h). The reaction mixture was worked up as above. The residue obtained from the ethyl acetate layer was chromatographed over silica gel (100–200 mesh) to obtain the mono-*p*-toluate **9** (eluent, ethyl acetate/light petroleum, 10:90 v/v, 0.064 g, 46%), the diol **7** (eluent, ethyl acetate/light petroleum, 20:80 v/v, 0.080 g, 67%) and the diester **8** (0.014 g, 14%). The aqueous layer was acidified with hydrochloric acid and extracted with ethyl acetate. The organic extract was dried over anhydrous sodium sulfate and evaporated to obtain *p*-toluic acid (0.013 g, 19%).

Reaction between 7 and 8 in solution: Diol **7** (0.032 g, 0.2 mmol), diester **8** (0.040 g, 0.1 mmol), sodium carbonate (0.085 g, 0.8 mmol) and dry *p*-xylene (2.5 mL) were heated (125°C) for 24 h. Excess of dry *p*-xylene (2.5 mL) was added and the heating continued for further 36 h. The reaction mixture was concentrated under reduced pressure and the residue worked up as above. Column chromatographic separation yielded **8** (0.016 g, 40%) and the monotoilate **9** (0.005 g, 9%). Use of dry DMF (instead of *p*-xylene) as the solvent for the same reaction resulted predominantly in the hydrolysis of **8** and formation of **9** was not observed.

DSC analysis: DSC curves for the co-crystal **7·8**, a 2:1 mixture of **7** and **8**, as well as **7**, were recorded on a Mettler Differential Scanning Calorimeter. Crystals (≈ 3 mg) were placed in a sealed aluminium pan (40 μL) and were analyzed from 45–175°C using an empty pan as the reference. The heating rate was 5°C min^{-1} and nitrogen gas was used for purging. The DSC curve for **7·8** showed a small and broad endothermic hump just above 120°C suggesting minor structural phase transition before the melting endotherm observed at 139.5°C (Figure S12, the Supporting Information).

X-ray crystallography: Single-crystal X-ray intensity measurements for co-crystal **7·8** at different temperatures and crystals of **9** at 25°C were recorded on a Bruker SMART APEX II and SMART APEX I single-crystal X-ray CCD diffractometer, respectively, with graphite-monochromatized ($\text{MoK}\alpha = 0.71073 \text{ \AA}$) radiation. The X-ray generator was operated at 50 kV and 30 mA. Diffraction data were collected with a ω scan width of 0.3° for **9** (φ settings 0, 90, 180, and 270°; the detector position (2θ) was fixed at -28°) and 0.5° for **7·8** (at different settings of φ and 2θ). The sample-to-detector distance was fixed at 6.145 cm for **9** and 5.00 cm for **7·8**. The X-ray data acquisition was monitored by SMART (for **9**)^[61] or APEX II (for **7·8**) programs.^[62] All the data were corrected for Lorentz-polarization and absorption effects using SAINT and SADABS programs integrated in APEX II program package.^[62] The structures were solved by the direct method and refined by full matrix least squares, based on F^2 , using SHELX-97^[63] (Table S1, the Supporting Information). Molecular diagrams were generated by using ORTEP-32.^[64] Geometrical calcula-

tions were performed using SHELXTL and PLATON.^[65] All the hydrogen atoms in the structure of **7-8** determined at -173°C were obtained from difference Fourier and refined isotropically. In structure of **7-8** determined at room temperature (25°C), hydrogen atoms bound to naphthalene ring were located in the difference Fourier map and refined isotropically. Hydrogen atoms bound to two hydroxyls that is, H1A, H2A were constrained to an ideal geometry ($\text{O-H}=0.82\text{ \AA}$ and $U_{\text{iso}}(\text{H})=1.5 U_{\text{eq}}(\text{O})$), whereas the H-atoms associated with benzene rings (H18, H19, H21, H22) and methyl groups (H23A, H23B, H23C) of the diester **8** were constrained to an ideal geometry ($\text{C-H}=0.93\text{ \AA}$ and $U_{\text{iso}}(\text{H})=1.2 U_{\text{eq}}(\text{C})$) for the phenyl H atoms and $\text{C-H}=0.96\text{ \AA}$ and $U_{\text{iso}}(\text{H})=1.5 U_{\text{eq}}(\text{C})$ for the methyl H-atoms). All the H-atoms in the structure determined at 125°C were placed in geometrically idealized position ($\text{O-H}(\text{OH})=0.82\text{ \AA}$, $\text{C-H}(\text{phenyl})=0.93\text{ \AA}$ and $\text{C-H}(\text{methyl})=0.96\text{ \AA}$) and constrained to ride on their parent atoms ($U_{\text{iso}}(\text{H})=1.5 U_{\text{eq}}(\text{O})$) for the hydroxyl H atom, $U_{\text{iso}}(\text{H})=1.2 U_{\text{eq}}(\text{C})$ for the phenyl H-atoms and $U_{\text{iso}}(\text{H})=1.5 U_{\text{eq}}(\text{C})$ for the methyl H atoms). In the structure of the co-crystal **7-8**, which was heated to 136°C and cooled to room temperature (25°C) for data measurement, the H atoms, such as H1A, H2A, H19, H21, H23A, H23B, and H23C were placed in geometrically idealized positions ($\text{O-H}(\text{OH})=0.82\text{ \AA}$, $\text{C-H}(\text{phenyl})=0.93\text{ \AA}$ and $\text{C-H}(\text{methyl})=0.96\text{ \AA}$) and constrained to ride on their parent atoms ($U_{\text{iso}}(\text{H})=1.5 U_{\text{eq}}(\text{O})$) for the hydroxyl H atom, $U_{\text{iso}}(\text{H})=1.2 U_{\text{eq}}(\text{C})$ for the phenyl H-atoms and $U_{\text{iso}}(\text{H})=1.5 U_{\text{eq}}(\text{C})$ for the methyl H atoms), whereas the remaining H-atoms were located in the difference Fourier map and refined isotropically. The hydroxyl hydrogen atom (H2A) in **9** was located in the difference Fourier map and refined isotropically; all the other hydrogen atoms were placed in geometrically idealized positions ($\text{C-H}(\text{phenyl})=0.93\text{ \AA}$ and $\text{C-H}(\text{methyl})=0.96\text{ \AA}$) and constrained to ride on their parent atoms ($U_{\text{iso}}(\text{H})=1.2 U_{\text{eq}}(\text{C})$) for the phenyl H-atoms and $U_{\text{iso}}(\text{H})=1.5 U_{\text{eq}}(\text{C})$ for the methyl H atoms). The thermal motion analysis of reactants in co-crystal **7-8** at different temperatures were carried out using anisotropic displacement parameters (ADP's) through the THMA11 program integrated in WinGX package.^[66] The program calculates the quantity $\Delta_{\text{A,B}}=Z_{\text{AB}}^2-Z_{\text{BA}}^2$ along any inter atomic vector AB (Z_{AB}^2 is the mean square displacement amplitude (MSDA)) of atom A in the direction of atom B.

Powder X-ray diffraction (PXRD) analysis: PXRD patterns were recorded on PANalytical X'PERT PRO instrument at a continuous scanning rate of $2^{\circ} 2\theta\text{min}^{-1}$ using $\text{Cu}_{\text{K}\alpha}$ radiation (40 kV, 30 mA) with the intensity of the diffracted X-ray being collected at intervals of $0.017^{\circ} 2\theta$. A nickel filter was used to remove $\text{Cu}_{\text{K}\beta}$ radiation. The PXRD pattern of the mixture of co-crystals **7-8** and solid sodium carbonate obtained by grinding them together revealed presence of diffraction peaks of individual components, that is, of **7-8** and sodium carbonate, thus eliminating the possibility of generation of any new crystalline phase during grinding (Figures S14 and S15, the Supporting Information).

Acknowledgements

M.I.T. and S.K. thank the CSIR, New Delhi for fellowships. Technical help from Niharika Pedireddi and helpful discussion with Dr. Mohan M. Bhadbhade are much appreciated. We thank Mangesh Mahajan for recording the PXRD patterns. This work was supported by the Department of Science & Technology (DST), New Delhi.

- [1] V. Ramamurthy, K. Venkatesan, *Chem. Rev.* **1987**, *87*, 433–481.
- [2] Y. Ohashi, *Reactivity in Molecular Crystals*, Wiley-VCH, Weinheim **1993**.
- [3] H. Kanazawa, Y. Ohashi, *Mol. Cryst. Liq. Cryst.* **1996**, *277*, 45–54.
- [4] I. Rubinstein, G. Clodic, G. Bolbach, I. Weissbuch, M. Lahav, *Chem. Eur. J.* **2008**, *14*, 10999–11009.
- [5] A. E. Keating, M. A. Garcia-Garibay, *Mol. Supramol. Photochem.* **1998**, *2*, 195–248.
- [6] D. Braga, F. Grepioni, *Angew. Chem.* **2004**, *116*, 4092–4102; *Angew. Chem. Int. Ed.* **2004**, *43*, 4002–4011.

- [7] A. E. Troup, H. Mitchner, *J. Pharm. Sci.* **1964**, *53*, 375–379.
- [8] A. L. Jacobs, A. E. Dilatush, S. Weinstein, J. J. Windheuser, *J. Pharm. Sci.* **1966**, *55*, 893–895.
- [9] K. T. Koshy, A. E. Troup, R. N. Duvall, R. N. Conwell, L. L. Shankle, *J. Pharm. Sci.* **1967**, *56*, 1117–1121.
- [10] R. S. Sardessai, S. Krishnaswamy, M. S. Shashidhar, *CrystEngComm* **2012**, *14*, 8010–8016.
- [11] M. D. Cohen, G. M. J. Schmidt, *J. Chem. Soc.* **1964**, 1996–2000.
- [12] M. D. Cohen, G. M. J. Schmidt, F. I. Sonntag, *J. Chem. Soc.* **1964**, 2000–2013.
- [13] G. M. J. Schmidt, *J. Chem. Soc.* **1964**, 2014–2021.
- [14] L. R. MacGillivray, G. S. Papaefstathiou, T. Frišćić, D. Varshney, T. D. Hamilton, *Top. Curr. Chem.* **2005**, *248*, 201–221.
- [15] J. Yang, M. B. Dewal, S. Profeta Jr., M. D. Smith, Y. Li, L. S. Shimizu, *J. Am. Chem. Soc.* **2008**, *130*, 612–621.
- [16] L. R. Macgillivray, G. S. Papaefstathiou, T. Frišćić, T. D. Hamilton, D.-K. Bucar, Q. Chu, D. B. Varshney, I. G. Georgiev, *Acc. Chem. Res.* **2008**, *41*, 280–291.
- [17] M. W. Ghosn, C. Wolf, *J. Org. Chem.* **2010**, *75*, 6653–6659.
- [18] M. H. Mir, L. L. Koh, G. K. Tan, J. J. Vittal, *Angew. Chem.* **2010**, *122*, 400–403; *Angew. Chem. Int. Ed.* **2010**, *49*, 390–393.
- [19] A. Gavezzotti, M. Simonetta, *Nouv. J. Chim.* **1978**, *2*, 69–72.
- [20] P. Venugopalan, K. Venkatesan, J. Klausen, E. Novotny-Bregger, C. Leumann, A. Eschenmoser, J. D. Dunitz, *Helv. Chim. Acta* **1991**, *74*, 662–669.
- [21] R. Sekiya, K. Kiyooka, T. Imakubo, K. Kobayashi, *J. Am. Chem. Soc.* **2000**, *122*, 10282–10288.
- [22] K. Tanaka, A. Tomomori, J. L. Scott, *Eur. J. Org. Chem.* **2003**, 2035–2038.
- [23] K. M. Sureshan, T. Murakami, T. Miyasou, Y. Watanabe, *J. Am. Chem. Soc.* **2004**, *126*, 9174–9175.
- [24] M. L. Cheney, G. J. McManus, J. A. Perman, Z. Wang, M. J. Zawortko, *Cryst. Growth Des.* **2007**, *7*, 616–617.
- [25] A. J. Gordon, *Tetrahedron* **1967**, *23*, 863–870.
- [26] K. Vyas, H. Manohar, K. Venkatesan, *J. Phys. Chem.* **1990**, *94*, 6069–6073.
- [27] T. Praveen, U. Samanta, T. Das, M. S. Shashidhar, P. Chakrabarti, *J. Am. Chem. Soc.* **1998**, *120*, 3842–3845.
- [28] C. Murali, M. S. Shashidhar, R. G. Gonnade, M. M. Bhadbhade, *Chem. Eur. J.* **2009**, *15*, 261–269.
- [29] M. P. Sarmah, R. G. Gonnade, M. S. Shashidhar, M. M. Bhadbhade, *Chem. Eur. J.* **2005**, *11*, 2103–2110.
- [30] S. Krishnaswamy, R. G. Gonnade, M. S. Shashidhar, M. M. Bhadbhade, *CrystEngComm* **2010**, *12*, 4184–4197.
- [31] S. Krishnaswamy, M. S. Shashidhar, M. M. Bhadbhade, *CrystEngComm* **2011**, *13*, 3258–3264.
- [32] H. B. Bürgi, J. D. Dunitz, *Acc. Chem. Res.* **1983**, *16*, 153–161.
- [33] D. R. Storm, D. E. Koshland, *J. Am. Chem. Soc.* **1972**, *94*, 5815–5825.
- [34] M. L. Bender, *Chem. Rev.* **1960**, *60*, 53–113.
- [35] I. Weissbuch, L. Leiserowitz, M. Lahav, *Top. Curr. Chem.* **2005**, *259*, 123–165.
- [36] G. R. Desiraju, T. Steiner, *The Weak Hydrogen Bond in Structural Chemistry and Biology*, Oxford University Press, Oxford, **1999**.
- [37] J. Bernstein, M. C. Etter, L. Leiserowitz in *Structure Correlation: The Role of Hydrogen Bonding in Molecular Assemblies, Vol. 1* (Eds.: H. B. Bürgi, J. D. Dunitz), Wiley-VCH, Weinheim, **2008**, pp. 431–507.
- [38] M. Nishio, Y. Umezawa, K. Honda, S. Tsuboyama, H. Suezawa, *CrystEngComm* **2009**, *11*, 1757–1788.
- [39] R. Boese, T. Clark, A. Gavezzotti, *Helv. Chim. Acta* **2003**, *86*, 1085–1100.
- [40] M. Chino, K. Nishikawa, T. Tsuchida, R. Sawa, H. Nakamura, K. T. Nakamura, Y. Muraoka, D. Ikeda, H. Naganawa, T. Sawa, T. Takeuchi, *J. Antibiot.* **1997**, *50*, 143–146.
- [41] K. Tanaka, D. Fujimoto, A. Altreuther, T. Oeser, H. Irngartinger, F. Toda, *J. Chem. Soc. Perkin Trans. 2* **2000**, 2115–2120.
- [42] S. Nakamatsu, K. Yoshizawa, S. Toyota, F. Toda, I. Matijasic, *Org. Biomol. Chem.* **2003**, *1*, 2231–2234.

- [43] S. A. Talipov, B. T. Ibragimov, K. M. Beketov, K. D. Praliev, T. F. Aripov, *Kristallografiya (Crystallogr. Rep.)* **2004**, *49*, 841–843.
- [44] K. Ghosh, M. Datta, R. Frohlich, N. C. Ganguly, *J. Mol. Struct.* **2005**, *737*, 201–206.
- [45] H.-Y. Peng, C. K. Lam, T. C. W. Mak, Z. Cai, W.-T. Ma, Y.-X. Li, H. N. C. Wong, *J. Am. Chem. Soc.* **2005**, *127*, 9603–9611.
- [46] J.-B. Yu, S.-W. Chen, G.-R. Zheng, L.-Y. Dai, *Acta Crystallogr. Sect. E: Struct. Rep.* **2008**, *64*, o1653.
- [47] G. A. Wallace, T. D. Gordon, M. E. Hayes, D. B. Konopacki, S. R. Fix-Stenzel, X. Zhang, P. Grongsaard, K. P. Cusack, L. M. Schaffter, R. F. Henry, R. H. Stoffel, *J. Org. Chem.* **2009**, *74*, 4886–4889.
- [48] E.-Y. Xia, J. Sun, R. Yao, C.-G. Yan, *Tetrahedron* **2010**, *66*, 3569–3574.
- [49] S. Varughese, G. R. Desiraju, *Cryst. Growth Des.* **2010**, *10*, 4184–4196.
- [50] A. Gavezzotti, *Acc. Chem. Res.* **1994**, *27*, 309–314.
- [51] T. Friščić, S. L. Childs, S. A. A. Rizvi, W. Jones, *CrystEngComm.* **2009**, *11*, 418–426.
- [52] R. Kuroda, J. Yoshida, A. Nakamura, S. Nishikiori, *CrystEngComm* **2009**, *11*, 427–432.
- [53] T. Friščić, W. Jones, *Cryst. Growth Des.* **2009**, *9*, 1621–1637.
- [54] D. P. McNamara, S. L. Childs, J. Giordano, A. Iarriccio, J. Cassidy, M. S. Shet, R. Mannion, E. O'Donnell, A. Park, *Pharm. Res.* **2006**, *23*, 1888–1897.
- [55] S. Basavoju, D. Bostrom, S. P. Velaga, *Pharm. Res.* **2008**, *25*, 530–541.
- [56] D. Daurio, C. Medina, R. Saw, K. Nagapudi, F. Alvarez-Núñez, *Pharmaceutics* **2011**, *3*, 582–600.
- [57] T. Friščić, W. Jones, *J. Pharm. Pharmacol.* **2010**, *62*, 1547–1559.
- [58] T. Itoh, T. Suzuki, T. Uno, M. Kubo, N. Tohnai, M. Miyata, *Angew. Chem.* **2011**, *123*, 2301–2304; *Angew. Chem. Int. Ed.* **2011**, *50*, 2253–2256.
- [59] D. H. Oswald, C. R. Pulham, *CrystEngComm.* **2008**, *10*, 1114–1116.
- [60] J. Bernstein, J. J. Novoa, R. Boese, S. Cirkel, *Chem. Eur. J.* **2010**, *16*, 9047–9055.
- [61] Bruker (2003), SADABS Version 2.05, SMART Version 5.631, and SAINT Version 6.45. Bruker AXS Inc., Madison, Wisconsin, USA.
- [62] Bruker (2006). APEX2, SAINT, and SADABS. Bruker AXS Inc., Madison, Wisconsin, USA.
- [63] G. M. Sheldrick, *Acta Cryst.* **2008**, *A64*, 112–122.
- [64] L. J. Farrugia, *J. Appl. Cryst.* **1997**, *30*, 565.
- [65] A. L. Spek, *J. Appl. Cryst.* **2003**, *36*, 7–13.
- [66] L. J. Farrugia, *J. Appl. Cryst.* **1999**, *32*, 837–838.

Received: March 19, 2013

Revised: May 29, 2013

Published online: August 9, 2013